Sub-cellular Feature Detection and Automated Extraction of Collocalized Actin and Myosin Regions

Justin Martineau
University of Maryland
Baltimore County
1000 Hilltop Circle
Baltimore, MD 21250
410-455-6338
jm1@umbc.edu

Ronil Mokashi
University of Maryland
Baltimore County
1000 Hilltop Circle
Baltimore, MD 21250
410-455-2860
ronil1@umbc.edu

David Chapman
University of Maryland
Baltimore County
1000 Hilltop Circle
Baltimore, MD 21250
410-455-6338
dchapm2@umbc.edu

Michael Grasso
University of Maryland School of Medicine
100 S. Paca Street, 6th Floor, #200
Baltimore, MD 21201
MikeGrasso@umbc.edu

Mary Brady
National Institute of Standards and Technology
100 Bureau Drive
Gaithersburg, MD
301-975-4094
mary.brady@nist.gov

Yelena Yesha
University of Maryland
Baltimore County
1000 Hilltop Circle
Baltimore, MD 21250
410-455-3542
yeyesha@cs.umbc.edu

Yaacov Yesha
University of Maryland
Baltimore County
1000 Hilltop Circle
Baltimore, MD 21250
410-455-2669
yayesha@cs.umbc.edu

Antonio Cardone
University of Maryland
Institute for Advanced Computer Studies
AVW Building
College Park, MD 20742
301-975-4463
cardone@nist.gov

Alden Dima
National Institute of Standards and Technology
100 Bureau Drive
Gaithersburg, MD
301-975-2450
alden.dima@nist.gov

ABSTRACT

We describe a new distance-based metric to measure the strength of collocalization in multi-color microscopy images for user-selected regions. This metric helps to standardize, objectify, quantify, and even automate light microscopy observations. Our new algorithm uses this metric to automatically identify and annotate a donut shaped actomyosin stress fiber bundle evident in vascular smooth muscle cells on certain types of surfaces. Both the metric and the algorithm have been implemented as an open source plugin for the popular ImageJ toolkit. They are available for download at `http://code.google.com/p/actin-myosin-plugin/`. Using cells stained for the cytoskeletal proteins actin and myosin, we show how characteristics of the identified stress fiber bundle are indicative of the kind of surface the cell is placed upon, and prove that weak spots in this structure are correlated with local membrane extensions. Given the relationship between membrane extension, cell migration, vascular disease, embryonic development, and cancer metastasis we provide that these tools to enable biological research that could improve our quality of life.

IHI'12, January 28–30, 2012, Miami, Florida, USA.

1. INTRODUCTION AND RELATED WORK

This study introduces a metric to standardize, quantify, and objectify light microscopy colocalization observations. It is important to standardize light microscopy colocalization observations observations so biologists can quickly, and robustly compare cells and subcellular regions. With standard metrics for colocalization we can define algorithms to automatically identify structural features in cells. For example, in Figure 1 there is an interesting stretched donut shaped actomyosin stress fiber bundle as annotated in blue in Figure 2. Algorithms that can identify these structural sub-cellular features coupled with metrics to determine their strength provide useful insights into cell migration, which is central to many vital biological processes, including vascular disease, embryonic development, and cancer metastasis.

To understand cell migration we examine the correlation between cytoskeletal organization and cell morphological features such as membrane protrusions. Membrane protrusions are structures that extend from the cell surface and are good indicators for cell migration. The areas roughly indicated in blue from Figure 4 are examples of membrane protrusions in our dataset. The cytoskeleton is a three-dimensional network of structural fibers found within the cytoplasm of a cell. It is responsible for cell movement and shape stability. Actin microfilaments (shown in red) are one of the three major types of fibers that form the cell cytoskeleton. Through their association with the motor protein myosin (shown in green) these microfilaments carry out cellular movements including gliding, contraction, and cytokinesis. Cells can sense and respond to the mechanical stiffness and the chemical identity of the surfaces that they attach to.

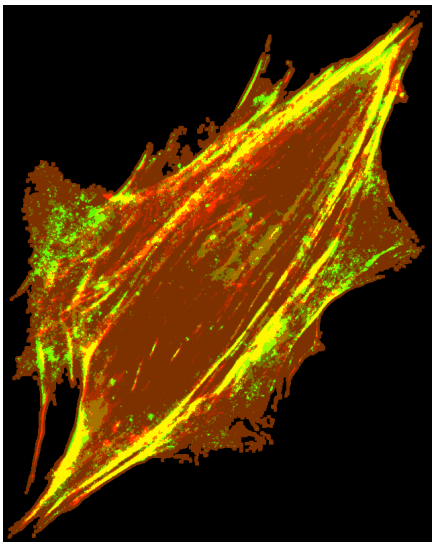

Figure 1: Smooth muscle cell with a stretched donut shaped actomyosin stress fiber bundle. Actin is stained in red. Myosin is stained in green. Yellow areas are overlapping actin and myosin.

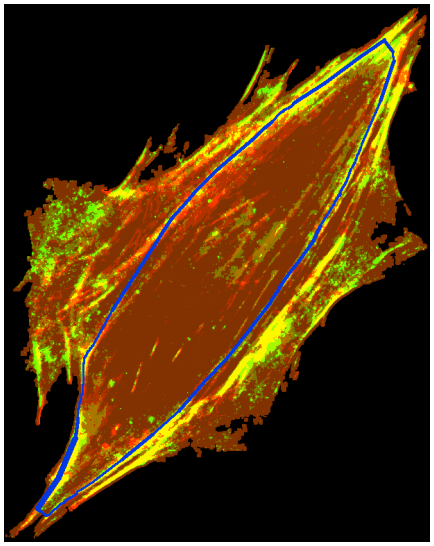

Figure 2: The structure we want to identify has been labeled and superimposed in blue upon the actomyosin stress fiber bundle.

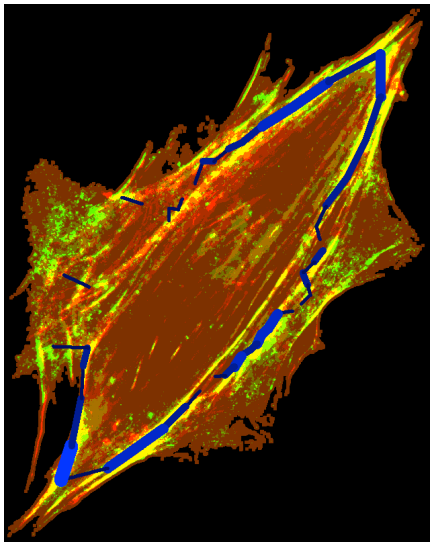

Figure 3: The proposed structure produced by our algorithm is annotated in blue. Thicker and brighter shades of blue represent higher metric scores indicating greater structure strength.

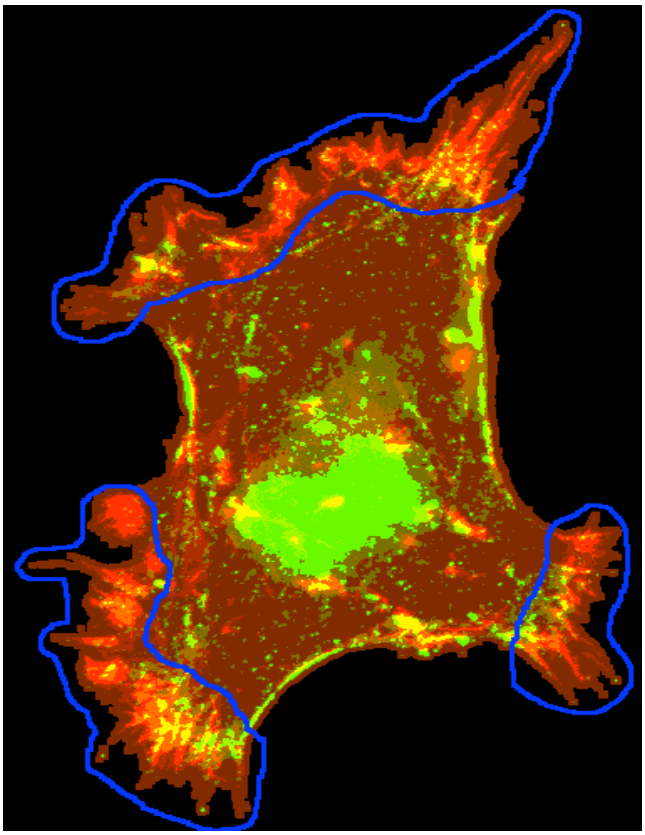

Figure 4: Membrane protrusions are circled in blue.

Light microscopy is a powerful approach to study cytoskeletal responses to the extracellular matrix because the cytoskeleton encodes for underlying signals from the extracellular matrix it rests on. Cell microscopy methods often involve the visual inspection of nuclei, organelles, and morphology. Using this approach, observations are made based on variations in cells from their expected appearance. However, this approach requires human judgments which are subjective due to observer variability, a lack of standardization, and a limited feature set.

Consequently, we define a set of quantitative measures that correlate well with the visual appearance of cells and that allow for both intracellular and intercellular comparisons to address this subjectivity. While there are many different statistical measures of dependence and correlation, this is the first measure of correlation or dependence for items adhering to a geometric structure. This kind of measure provides a new kind of information that can improve computational image classification accuracy. Computational image classification techniques have been successfully applied to a number of clinical problems [5] [4] [2].

Computational image classification is used to categorize a raster image into a finite set of classes based on computationally extracted features. When considering meaningful features for describing an image, the three fundamental features include spectral, textural, and contextual features. Spectral features describe the tonal variations that can be measured as a distribution and represented as a histogram [9]. Textural features contain information about the spatial distribution of tonal variations. These tonal variations can be represented as a co-occurrence matrix [8]. The first two types of features, spectral and textural, are essentially non-geometric image features based on tonal variations and tonal distributions. Contextual features are more complex. They are used to extract structural information from the image context. This paper defines new structural features for image retrieval, classification, and other kinds of analysis building on our previous work in this area [7].

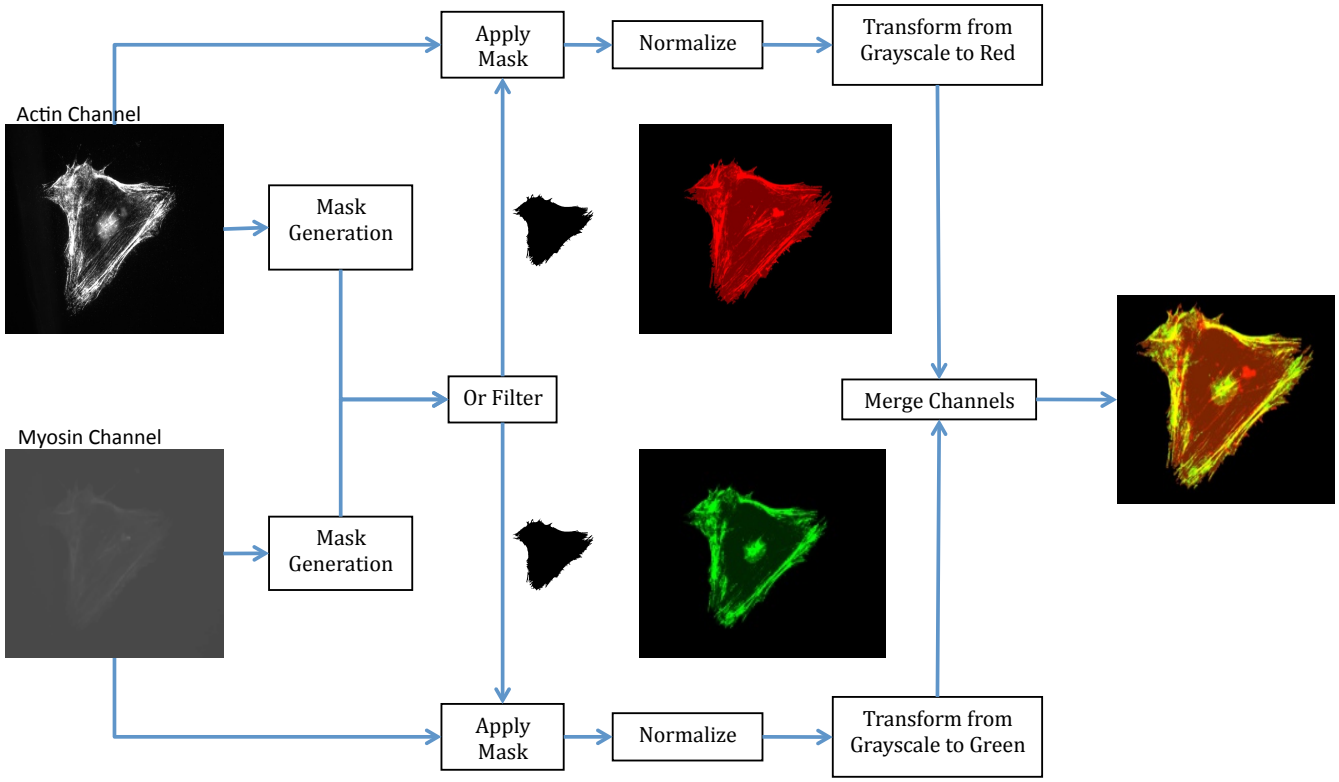

Figure 5: Visualize Cell Overview

The image processing and feature extraction algorithm is available for download as an ImageJ plugin at `http://code.google.com/p/actin-myosin-plugin/`. This plugin measures how well dual channel signals, such as actin and myosin, colocate with distance from a region of interest. This plugin uses a new metric we developed to measure the correlation between two channels in 2-D space as the distance from a specified region grows. This metric will help biologists quantify visual judgments about structural features both within a cell and between other cells.

Our experiments are on the A10 cell line, rat aortic vascular smooth muscle cells. The polarity of a cell, as defined by its functional and morphological asymmetry, is an important function in cell growth and differentiation [11]. This polarity reflects in part cell interactions with the extracellular matrix. These interactions are accomplished by both receptor-dependent interactions and also by the mechanical stiffness of the extracellular matrix. Our specific interest is on the regulation of vascular smooth muscle cells by the mechanical stiffness of arteries [6] [10] . To examine this phenomenon, we experimentally manipulated the underlying matrix stiffness in order to gain insights into the resulting cell morphogenesis. We placed cells onto the following four different surfaces: mechanically stiff collagen, mechanically flexible collagen, monolayer collagen, and fibronectin. After 24 hours the cells were fixed and stained with reagents for actin and myosin proteins, and acquired using light microscopy. The procedure for fixing the cells is the same procedure we used in our prior work on automated fluorescence microscopy [1]. The collagen thin films were made using the same methods described in our prior work on collagen fibrils [6] [10].

2. TOOLS

We provide two main tools as part of the plugin. The first tool processes dual channel two dimensional images to produce a visualization that allows biologists to see a spatial relationship and determine where the channels are strongest together. Figure 5 shows a flow chart detailing the process we use to create this visualization. Our second tool works on these processed images. It scores regions of interest based upon how far away the most intense overlapping signals are from the region. Regions of interest can be quickly specified using ImageJ's region of interest polygon tool. That tool allows users to place vertices with a point and click interface. Vertices can be moved by dragging them into place. Users can then run the "Band Score" tool. This allows users to painlessly make minor changes to their regions of interest if they so desire. Used in combination, these two plugins follow this general procedure:

1. Remove background from the raw images.
2. Normalize each color channel image independently.
3. Combine the two color channels.
4. Define the region of interest by placing vertices.
5. Score the region of interest.

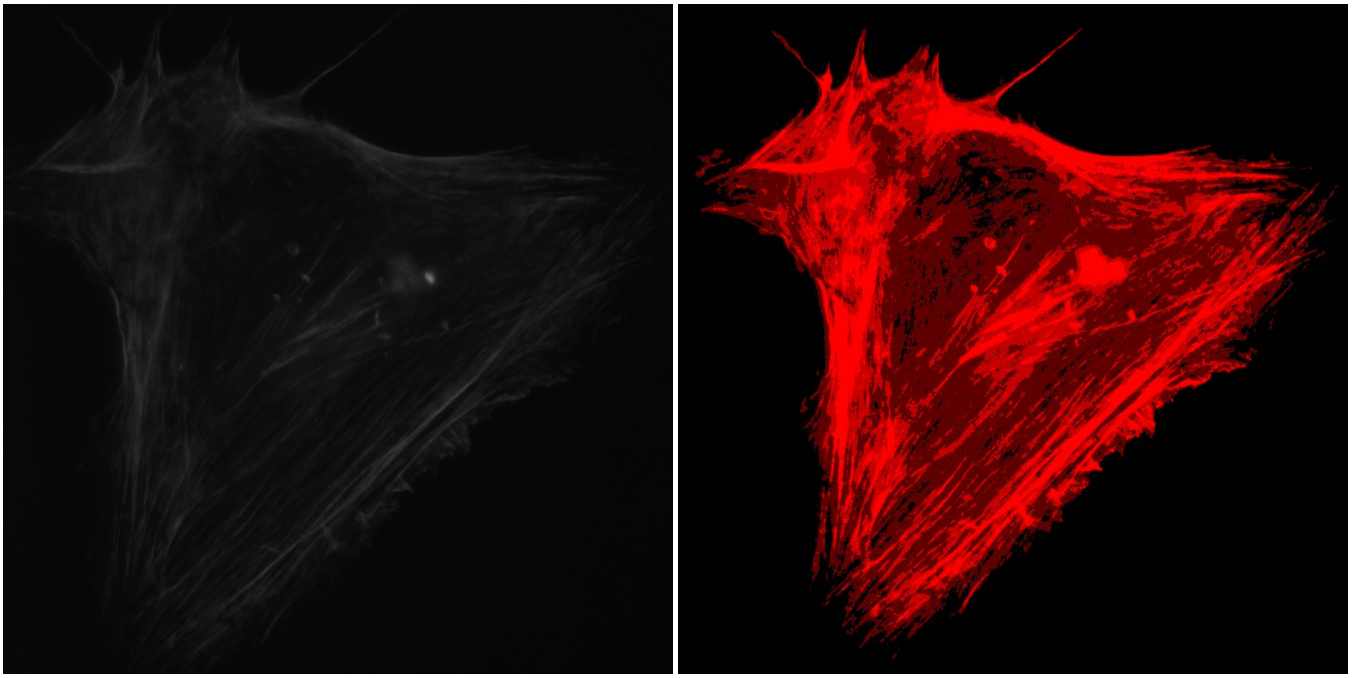

Figure 6: Actin channel grayscale image before and after normalization and color transformation

2.1 Remove Background

Before normalization it is important to remove pixels that are not part of the cell, because our normalization technique uses distributional knowledge about pixel values. By removing background pixels and pixels from nearby cells we can better measure the distribution of intensity values for the cell in question.

ImageJ already provides tools to do this. Our technique uses the *make binary*, *convert to mask*, and then *fill holes* plugins to create a mask. First we convert a copy of the image into a binary format. Using a morphological filtering process, we dilate the binary image using a quasi-circular structuring element. Dilation with a circular element of radius R increases the width of the foreground cell structure by R. Then we use ImageJ's Binary class to fill holes in 8-connected particles of the cell mask. Using ImageJ's *Analysis* class we find the largest particle in the image. This particle is retained as a cell mask and other smaller artifacts are merged with the background.

We create these masks for both the red channel image and the green channel image. We produce a final mask using an "or" function. If either mask says the pixel is in the cell then the pixel is in the cell. Pixels that are outside of this mask are displayed in black. Every successive step checks this mask and does not operate on any pixels determined to be outside the cell.

2.2 Channel Normalization

In order to visualize the relative intensity of actin to myosin, biologists normally apply contrast enhancement algorithms, and manually tune pixel thresholds and other settings. This process is manuel, highly subjective, and prone to errors and differences of opinion. A consistent automated normalization algorithm would alleviate these problems.

Instead of providing normalization algorithms ImageJ only provides "false color-scale transformations". These transformations map one set of pixel intensities to another using predefined "Black-Box" lookup tables that are completely independent of the data being used. Many of these transformations are hand-tuned and include optimizations for specific tasks.

Instead of using a fixed lookup table that is independent of our data points, we use V(p) in Equation 1. V(p) accounts for different distribution of colors within different images. It is possible for this normalization technique to transform the same raw intensity value from two different images into two different output colors based upon the distribution of colors in each of those images.

Given that:

$N-$	Number of bins
$R-$	Fraction of a standard deviation covered by a bin
$p-$	Raw pixel value
$X-$	Mean pixel value
$S-$	Size of 1 standard deviation
$O(p)-$	Offset in standard deviations from mean $= \frac{p-X}{S}$
$M-$	Max pixel value

$$V(p) = \begin{cases} 0 & \text{if } O(p) < -\frac{NR}{2} \\ \frac{M}{N}(\lfloor \frac{N}{2} + \frac{O(p)}{R} \rfloor + 1) & \text{if } -\frac{NR}{2} <= O(p) < \frac{NR}{2} \\ M & \text{if } O(p) >= \frac{NR}{2} \end{cases} \quad (1)$$

V(p) in Equation 1 converts raw pixel values to normalized intensity values for a given channel. We normalize the actin channel separately from the myosin channel. Once the actin

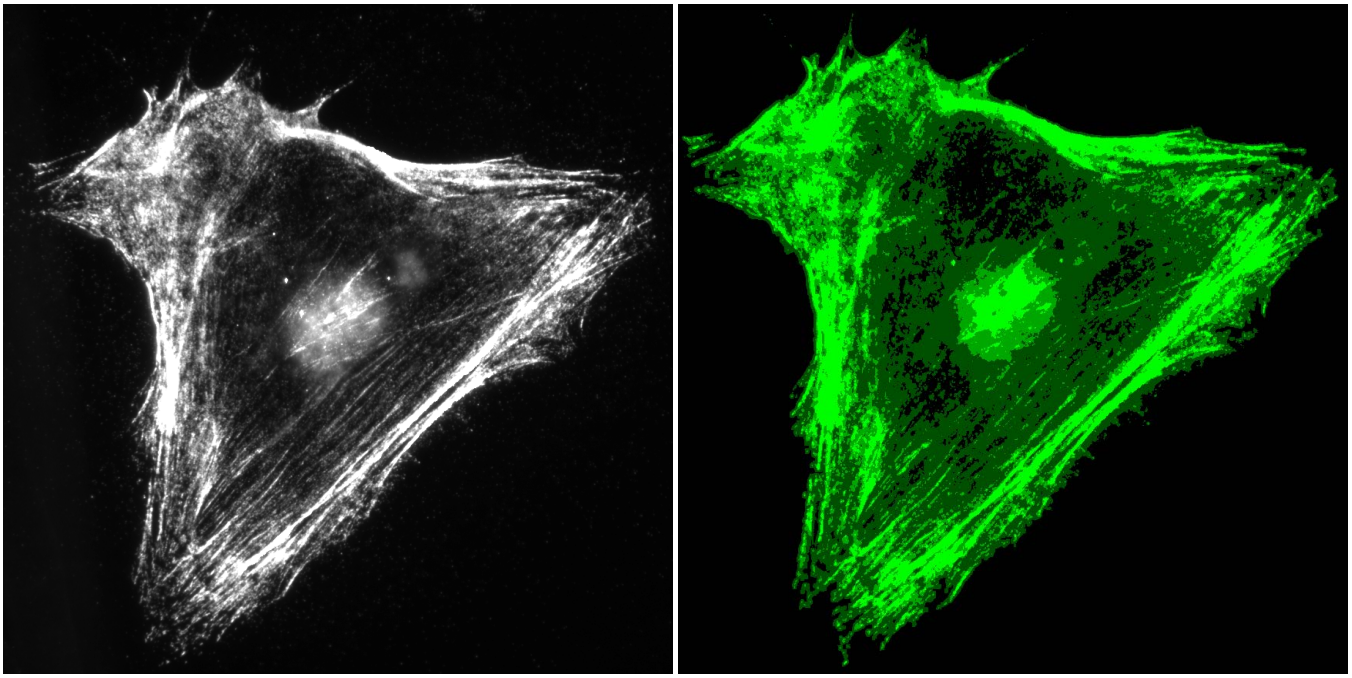

Figure 7: Myosin channel grayscale image before and after normalization and color transformation

and myosin color channels are normalized independently but to the same color scale, they are comparable and can be visualized without further hand tuning. To apply V(p) first, create a bin for each fraction "R" of a standard deviation from the mean "X" of the raw pixel values in the channel. Then determine which bin pixel "p" belongs to by calculating the offset "O(p)" of the pixel from the mean in standard deviations. The pixels in each bin all receive the same value for V(p). The range of output values for V(p) are linearly distributed per bin starting from the minimum pixel value 0 and ending at the maximum pixel value "M".

We normalize each channel by V(p) and plot the pixel intensities to a specified RGB color component. Figure 6 shows how the actin channel is normalized by V(p) and plotted as the Red color component. Figure 7 shows how the myosin channel is normalized by V(p) and plotted as the Green color component.

2.3 Merge Channels

ImageJ has standard tools to combine and overlay multiple images. After running our normalization algorithm we assign each grayscale image a color. In the experiments shown we used the red channel for the actin stain and the green channel for the myosin stain. We overlay these channels on top of each other and present them to the user as a single full color image. As shown in Figure 8 this results in yellow areas that reveal actin/myosin colocalization.

Brighter green colors indicate that myosin in that area has a stronger intensity than elsewhere in the cell. Likewise, brighter red colors indicate that actin in that area has a stronger intensity than elsewhere in the cell. Brighter yellow colors indicate stronger colocalization of actin and myosin. Black color indicates that neither actin or myosin is present, or that these signals are present at such low intensity values that they are placed in the bin representing the standard deviation farthest below the mean.

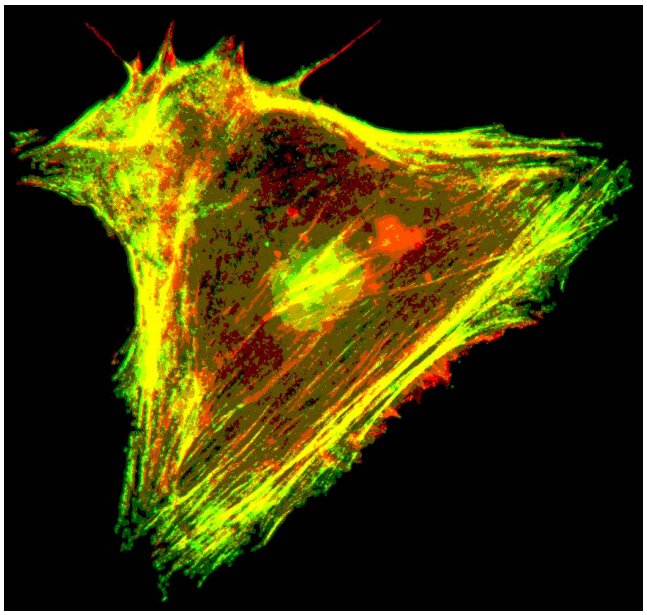

Figure 8: Cell after merging red and green.

Selecting the "Visualize Cell" function from the plugins menu will produce merged images, like that shown in Figure 8, using the two channels and the normalization parameters you specify.

2.4 Band Structure

Myosin is known to travel along Actin fibers during muscle movement. The overlap of actin and myosin forms meaningful shapes that define the cytoskeleton. Breaks in this structure are also significant and tend to indicate membrane protrusions. The relationship between membrane protrusions and cell motion is an interesting research question.

These actin/myosin colocations commonly form a band-like structure inside the cell roughly following the perimeter of the cell. A polygon can be defined to represent this structure. The polygon, it's geometric properties, and the distribution of actin and myosin along this polygon are measurable features that can be used to analyze and compare cells quantitatively.

2.5 Distance Based Collocation Metric

Users can annotate polygonal structures using our ImageJ plugin with the "Region of Interest" tool. The "Region of Interest" tool allows users to annotate a polygon by placing vertices in order around the cell. The "Score" plugin reports the strength of the actin/myosin colocation around the defined polygon, and annotates the edges by their relative strength. Later in the paper we introduce an algorithm to automatically define the polygon by optimizing the score metric.

The scoring function is a linear combination of all the pixels. Pixels have both a weight and a collocation value. Each pixel's weight is determined by how close it is to the band. The collocation value is set when the normalized intensity values of both the actin and myosin channels are at the maximum value "M" from function V(p). These pixels appear as completely bright yellow in our merged color representation, therefore we refer to them as "yellow" pixels. Pixel weight is proportional to the inverse of the distance of the pixel from the band raised to a power. This power can be set using the falloff constant. By default it is set to 2 resulting in the popular inverse square law.

The collocation value of each pixel is determined by the collocation of actin and myosin. If the pixel is "yellow", as defined above, then it has value 1 divided by the number of "yellow" pixels, otherwise it has value -1 divided by the number of other pixels. Thus pixels with high values of actin and myosin, relative to the rest of the cell, improve the band score while all other pixels degrade it. Normalizing the weight of a "yellow" pixel to the number of "yellow" pixels and the weight of non-yellow pixels to the number of non-yellow pixels places an equal value upon bands that can get the closest to all the yellow pixels and bands that avoid non-yellow areas. It is possible to multiply non-yellow pixels by an additional weight parameter to prefer or discourage matching yellow pixels over avoiding non-yellow pixels.

$$
\begin{aligned}
D(x,y)- &\quad \text{Minimum distance of pixel (x,y) to an edge} \\
F- &\quad \text{Falloff constant} \\
Y- &\quad \text{Number of yellow pixels} \\
N- &\quad \text{Number of non-yellow pixels} \\
C(x,y) = &\quad \begin{cases} 0 & \text{if pixel (x,y) is not yellow} \\ 1 & \text{if pixel (x,y) is yellow} \end{cases} \\
C'(x,y) = &\quad \begin{cases} 1 & \text{if pixel (x,y) is not yellow} \\ 0 & \text{if pixel (x,y) is yellow} \end{cases} \\
P(x,y) = &\quad \frac{\frac{C(x,y)}{Y} - \frac{C'(x,y)}{N}}{(D(x,y)+1)^F} \qquad (2)
\end{aligned}
$$

We create band scores by summing the weighted pixel values produced using Equation 2. For every pixel in the cell we determine the nearest band edge. This determines which edge that pixel will add its weight to. We then sum the pixel weights to determine the edge weights. The total band score is the sum of all the edge scores. This band is displayed on top of the cell using a blue line of variable width to indicate the relative strength of each segment of the band. Edges that are abnormally below average are considered breaks in the band and are not displayed. Edges that are no more than 1 standard deviations below the average edge score are displayed with increasing thickness starting with a 1 pixel width blue line. Each additional standard deviation above that increases the width of the line by 1 pixel.

2.6 Automatic Band Detection Algorithm

Polygons representing collocated actin/myosin stress fibre bands can be automatically defined. We provide an automatic band detection algorithm that identifies a band (donut shaped region) of actin collocated with myosin which commonly appears near the perimeter of vascular smooth muscle cells in our dataset. Our algorithm defines this band by intelligently placing vertices around the cell on the stress fibre band to be detected.

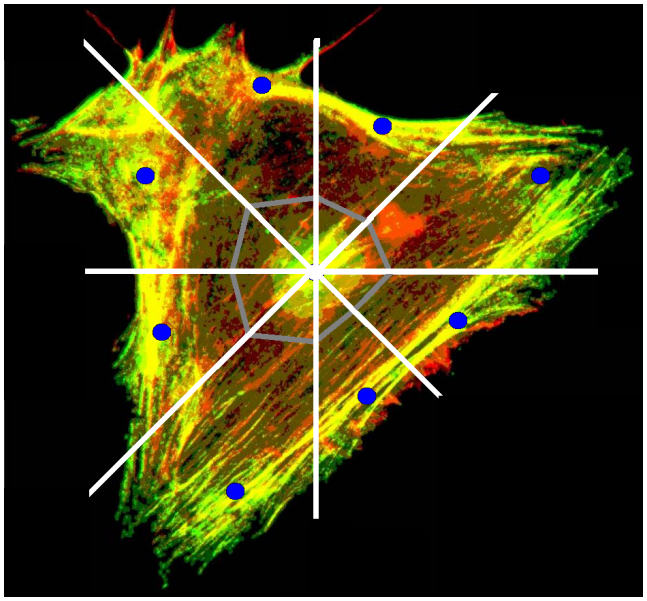

Figure 9: Hand made illustration of automatic vertex placement. White lines indicate radial segments or pie slices. Blue dots, representing vertices, are automatically placed at the center of mass of yellow pixels in the slice. Yellow pixels within the gray polygon are ignored.

The algorithm uses a radial coordinate system around the center of mass or "centroid" of the non-zero pixels in the normalized cell as shown in Figure 9. The cell is segmented into a tunable number of radially even bins or "pie slices". In each slice the algorithm attempts to place a vertex in the center of mass for "yellow" pixels within that slice with certain constraints. Firstly "yellow" pixels too near the centroid are discarded to discount interior actin/myosin structures (e.g. nucleus) unrelated to the stress fibre band. This threshold distance is a percentage (default 1/3) of the radius

of the current slice. Secondly, the vertex must be placed on a yellow pixel and near other yellow pixels, otherwise the detected actin/myosin fibre structure is too spurious to be considered part of the band. Should the vertex fail the second constraint, then a new vertex position is calculated by ignoring all "yellow" pixels that are closer to the centroid than the old vertex position. This last heuristic once again discounts the effects of non-band internal fibre structures.

3. EVALUATION

We used manual annotations by a biologist on normalized cells as our ground truth. The biologist used ImageJ to circle membrane projections. He also placed an "X" mark over locations were the band was noticeably discontinuous and/or where actin fibers appeared to splay off into the membrane projection. Large areas with a continuum of small breaks and extensions were considered as a single break and extension from the cytoskeletal band structure. Where there were multiple bands of cytoskeletal fibers running parallel to each other, only the one closest to the edge was considered in examining for breaks. The ends of the cell, of which there are typically two, were not marked for extensions or breaks. Geometrically, a cell end point is a region where stress fibers converge or nearly converge. To ensure high quality ground truth data, the cells were annotated a second time by the annotator a week later and conflicting annotations were removed. Using both sets of annotations we determined that the ground truth annotations for cells on monolayer and mechanically stiff collagen surfaces were stable enough to be used for further analysis.

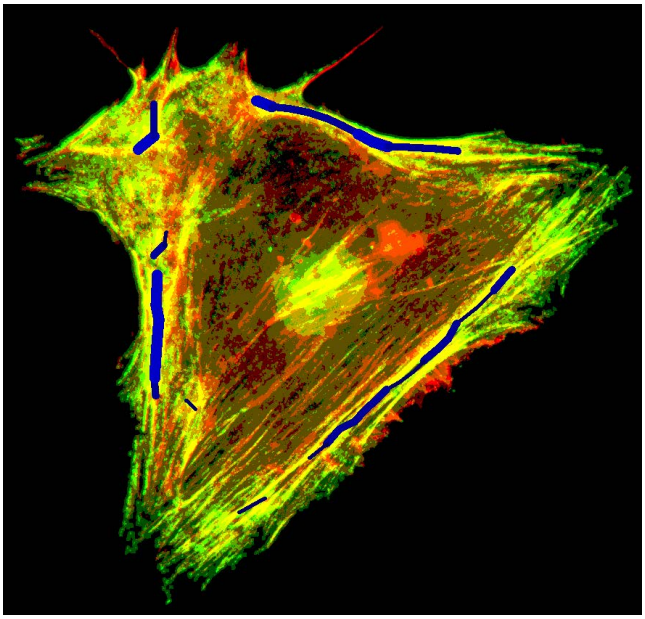

Figure 10: Automatic Band for a cell on mechanically stiff collagen after 24 hours.

Weak spots in the band tend to indicate membrane projections. To prove this statement we converted the ground truth into labels marking whether edges had a membrane extension on their exterior. Edges were judged as having an extension on their exterior if a line could be drawn from the membrane projection through the edge to the center of mass of the cell. Additionally, cell end points were counted as membrane extensions. We assigned a 1 to an edge if it had an extension on the outside and a 0 otherwise. We calculated the Pearson's Correlation Coefficient of these labels to our metric's score for those edges. Keep in mind that our metric can produce a negative score when non-yellow points outweigh nearby yellow points, indicating an abnormally weak edge. Using all our ground truth data we found a Pearson's Correlation of -0.4458 between edges with a strong band and edges that have a membrane extension. This proves our hypothesis that low metric scores correlate to nearby membrane extensions.

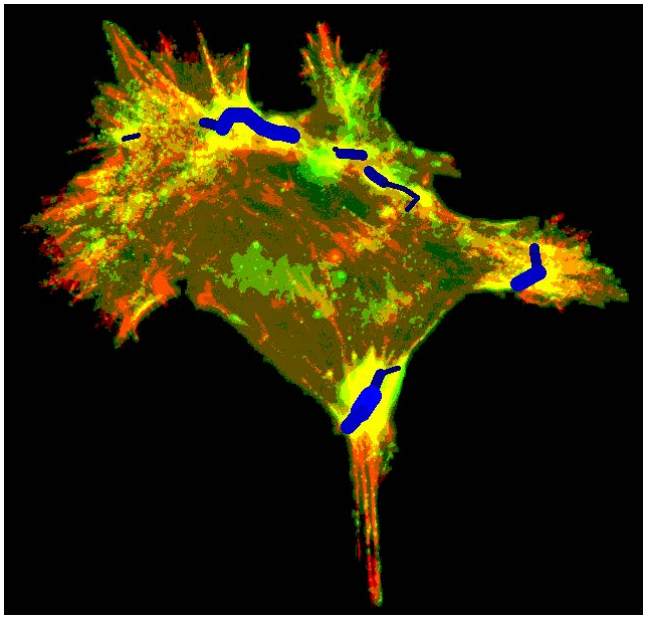

Figure 11: Automatic Band for a cell on mechanically flexible collagen after 24 hours.

Visual inspection of cells fixed on mechanically stiff collagen, mechanically flexible collagen, fibronectin, and monolayer collagen reveals that after 24 hours, cells on these different surfaces have very different shapes and structures. Cells on mechanically stiff collagen, like Figure 10, tend to be elliptical (or at least convex) exhibiting a reasonably well connected yellow band with a similar shape. This yellow band tends to be near the exterior of the cell.

Cells on flexible surfaces, such as the cell in Figure 11 placed on mechanically flexible collagen, do not have this kind of shape. Instead they tend to be concave with bright yellow regions inside the areas jutting out. These bright yellow regions are frequently not connected to each other by other yellow fibers. In about half of these cells yellow fibers project out from these yellow points in various directions.

Fibronectin is a much stiffer surface than mechanically stiff collagen [3]. Cells on fibronectin, such as the cell in Figure 12, tend to be more spread out. Within a cell, fibers tend to all be oriented in the same direction. It is similar to the way a board of lumber has a grain. There appears to be a band that travels along these fibers when they run parallel to the edge of the cell, but the band will run against the grain of these stress fibers if the cell exterior does. In the latter case, it looks like a fat yellow paintbrush was run lightly over a piece of wood going against the grain.

Cells on monolayer collagen, like Figure 13 tend to exhibit a c-shaped band.

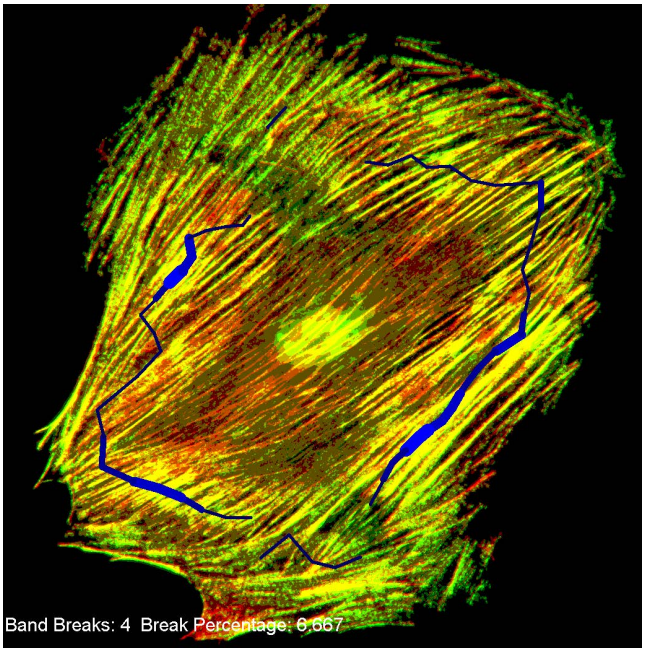

Figure 12: Automatic Band for a cell on Fibronectin after 24 hours.

It is possible to predict what type of surface a cell is located on using a simplified geometric representation for the network of structural fibers in the cell. We speculate that surface stiffness is a factor affecting the overall shape of structural fibers in a cell. To test this theory we built a classifier, using structural features, to distinguish between cells on each surface. Our structural features include the band score, the number of vertices successfully placed, the total number of continuous band breaks, the percentage of "yellow" pixels, what percentage of the cell the band covers, the strength of each edge in the band, and the length of the five largest breaks.

To improve classification accuracy we combined these structural features with the spectral and textural features used in prior image classification approaches [7]. We also included the mean and the size of a standard deviation for both the actin and myosin channels in our feature set. We trained a LogitBoost meta classifier in Weka using this feature set with a resulting classification accuracy of 92.8%. Without structural features accuracy drops to 85%. Clearly, structural features exhibited by a cell are an important component to consider when examining the interaction between a cell and the surface it is on.

4. FUTURE WORK

There are many possible directions to pursue from both the computer science and biological perspectives. Building a better algorithm to determine the band shape is an obvious extension. Using machine learning and artificial intelligence algorithms to improve membrane extension detection given the band and local features outside of the band is another promising research avenue. With time series data we could investigate the theory that weak areas in the band without membrane extensions at the current time are more likely to develop them in the future. Furthermore, time series data could help determine what direction cells are moving in and how the identified cytoskeletal features affect this movement.

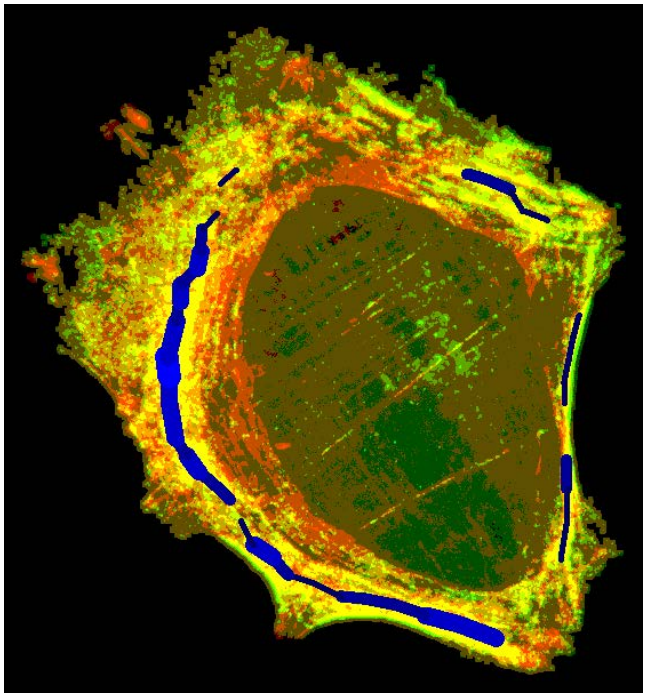

Figure 13: Automatic Band for a cell on monolayer collagen after 24 hours.

Our automatic structural identification algorithm could be used to facilitate structural image search. Designing a structural similarity metric for bands in conjunction with textual and spectral similarity metrics would make it possible to search for cells that are like a given cell. This kind of search could be very valuable for doctors treating infections, and for researchers looking for relevant publications on similar cells.

5. CONCLUSION

In this work we identified a cytoskeletal structure that commonly occurs in the A10 cell line on mechanically stiff collage, mechanically flexible collage, monolayer collage, and fibronectin. We designed a new metric and integrated it into a new algorithm to automatically identify and measure the strength of this structure. We implemented this measure in the popular ImageJ toolkit and made it available for download. Using these tools we determined that weak areas in this structure are correlated to membrane extensions. Furthermore, we showed that cells placed on different surfaces tend to exhibit a different general shape in the identified structure. These findings provide new insights and raise new question about membrane protrusion formation and cell migration.

6. ACKNOWLEDGEMENTS

We would like to thank Kiran Bhadriraju at NIST for providing us with the data used in this project, for annotating cells and providing our ground truth, for meeting with us many times, for pointing out an interesting problem, and for all the rest of his hard work on this project. Without Kiran this research would not be where it is today. Additionally, we would also like to thank Anne Plant at NIST for her leadership and other contributions to this project.

7. REFERENCES

[1] K. Bhadriraju, J. Elliott, M. Nguyen, and A. Plant. Quantifying myosin light chain phosphorylation in single adherent cells with automated fluorescence microscopy. *BMC Cell Biology*, 8(1):43, 2007.

[2] M. Boland and R. Murphy. A neural network classifier capable of recognizing the patterns of all major subcellular structures in fluorescence microscope images of HeLa cells. *Bioinformatics*, 17(12):1213, 2001.

[3] K. Chung, K. Bhadriraju, T. Spurlin, R. Cook, and A. Plant. Nanomechanical Properties of Thin Films of Type I Collagen Fibrils. *Langmuir*, 26(5):3629–3636, 2010.

[4] S. Doyle, S. Agner, A. Madabhushi, M. Feldman, and J. Tomaszewski. Automated grading of breast cancer histopathology using spectral clustering with textural and architectural image features. In *Biomedical Imaging: From Nano to Macro, 2008. ISBI 2008. 5th IEEE International Symposium on*, pages 496–499. IEEE, 2008.

[5] R. Eils and C. Athale. Computational imaging in cell biology. *The Journal of cell biology*, 161(3):477, 2003.

[6] J. Elliott, A. Tona, and A. Plant. Comparison of reagents for shape analysis of fixed cells by automated fluorescence microscopy. *Cytometry Part A*, 52(2):90–100, 2003.

[7] M. A. Grasso, R. Mokashi, D. Dalvi, A. Cardone, A. A. Dima, K. Bhadriraju, A. L. Plant, M. Brady, Y. Yesha, and Y. Yesha. Image classification of vascular smooth muscle cells. *IHI '10*, pages 484–486, 2010.

[8] R. Haralick, K. Shanmugam, and I. Dinstein. Textural features for image classification. *IEEE Transactions on systems, man and cybernetics*, 3(6):610–621, 1973.

[9] I. Kunttu, L. Lepisto, J. Rauhamaa, and A. Visa. Binary histogram in image classification for retrieval purposes. In *Intl. Conf. in Central Europe on Computer Graphics, Visualization and Computer Vision*, pages 269–273. Citeseer, 2003.

[10] D. McDaniel, G. Shaw, J. Elliott, K. Bhadriraju, C. Meuse, K. Chung, and A. Plant. The stiffness of collagen fibrils influences vascular smooth muscle cell phenotype. *Biophysical journal*, 92(5):1759–1769, 2007.

[11] M. Théry, V. Racine, M. Piel, A. Pépin, A. Dimitrov, Y. Chen, J. Sibarita, and M. Bornens. Anisotropy of cell adhesive microenvironment governs cell internal organization and orientation of polarity. *Proceedings of the National Academy of Sciences*, 103(52):19771, 2006.